SCALAR STATISTICS IN PREMIXED FLAME-WALL INTERACTION WITHIN TURBULENT BOUNDARY LAYERS UNDER DIFFERENT FLOW CONFIGURATIONS

Umair Ahmed[1,*], Sanjeev Kr. Ghai[1], Nilanjan Chakraborty[1], Markus Klein[2]

[1]School of Engineering, Newcastle University, Newcastle upon Tyne NE1 7RU, United Kingdom
[2]Department of Aerospace Engineering, Bundeswehr University Munich, Neubiberg, Germany

ABSTRACT

The influence of thermal wall boundary conditions on the behaviour of scalar statistics during flame-wall interaction (FWI) of premixed flames within turbulent boundary layers has been investigated. Three-dimensional direct numerical simulations (DNS) of two different flow configurations for flames interacting with chemically inert isothermal as well as adiabatic walls in fully developed turbulent boundary layers have been performed. The first configuration is an oblique wall interaction (OWI) of a V-flame in a turbulent channel flow and the second configuration is representative of head-on interaction (HOI) of a planar flame in a turbulent boundary layer. The turbulence in the non-reacting conditions for these simulations is representative of the friction velocity based Reynolds number of $Re_\tau = 110$. Differences in the mean behaviours of the progress variable and non-dimensional temperature have been observed for the two configurations in response to different wall boundary conditions. Mean scalar variance of the progress variable and temperature and their respective scalar dissipation rates have been investigated and it is found that the variances of the progress variable and temperature remain coupled in the case of adiabatic walls, while significant differences exist between these quantities in the vicinity of the wall under isothermal wall conditions for both flow configurations. The mean scalar dissipation rates of progress variable and temperature during FWI decrease towards the wall in both flow configurations under different thermal wall boundary conditions, but in the case of isothermal wall conditions a higher scalar dissipation rate for the non-dimensional temperature is observed when compared with the scalar dissipation rate for the progress variable.

1 INTRODUCTION

The combustors are increasingly being made more fuel efficient and smaller in size to increase energy density thus leading to events like flame-wall interaction (FWI) in many engineering devices including gas turbine engines and micro-combustors, and modelling these phenomena remains challenging. In FWI, combustion is strongly influenced by the presence of walls, which leads to flame quenching due to wall heat loss. Furthermore, the flame also has an influence on the flow near the wall as well as on the wall heat flux [1]. This leads to the turbulence structure being altered by the wall and the interaction of flame elements with walls leads to modifications of the underlying combustion processes which produce variations in the thermal load of the combustor walls [1]. In practice, limited information is available regarding the behaviour of turbulence and heat transfer processes during FWI in fully developed boundary layers. Thus, this paper focuses on the turbulent scalar statistics during FWI of premixed flames within fully developed turbulent boundary layers for isothermal and adiabatic wall boundary conditions using Direct Numerical Simulation (DNS) data.

1.1 Direct Numerical Simulation Data

In this work, DNS of two different flame configurations have been considered which represent methane-air combustion under unity Lewis number, stoichiometric and low Mach conditions. The first configuration consists of the oblique FWI of a V-flame with walls under isothermal and adiabatic conditions in a turbulent channel flow, while the second configuration consists of a statistically planar flame propagating into a fully developed turbulent boundary layer and interacting with the wall at isothermal and adiabatic

*Corresponding author: umair.ahmed@newcastle.ac.uk

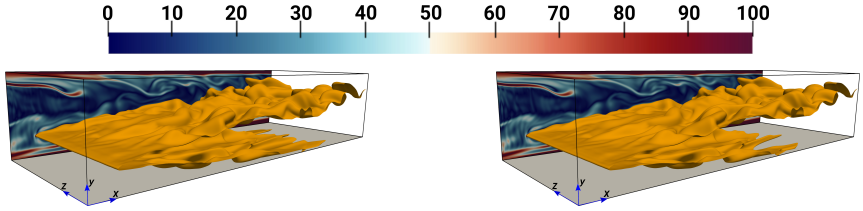

Isothermal Walls Adiabatic Walls

Figure 1: V-flame oblique wall interaction with isothermal wall boundary conditions (top) and with adiabatic wall boundary conditions (bottom). The isosurface coloured in yellow represents $c = 0.5$. The instantaneous normalised vorticity magnitude Ω is shown on the $x-y$ plane at $z/h = 4$. The grey surface denotes the bottom wall.

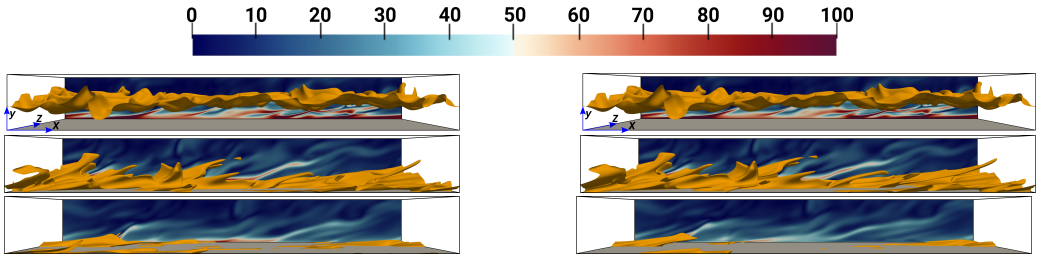

Isothermal Wall Adiabatic Wall

Figure 2: Head-on interaction with isothermal wall boundary conditions (left) and with adiabatic wall boundary conditions (right) at different time instants. From top to bottom $t/t_f = 4.20$, $t/t_f = 12.60$, $t/t_f = 14.70$. The isosurface coloured in yellow represents $c = 0.5$. The instantaneous normalised vorticity magnitude Ω is shown on the $x-y$ plane at $z/h = 4$. The grey surface denotes the wall.

conditions. A three-dimensional compressible DNS code SENGA+ [2, 3] has been used to perform these simulations. The code employs high-order schemes for spatial differentiation and time advancement. A single-step irreversible reaction is used to represent the combustion process. The initial turbulence conditions for both simulations and the inflow conditions for the V-flame simulation are obtained by performing an auxiliary DNS of inert fully developed turbulent-plane channel flow driven by a streamwise constant pressure gradient. The bulk Reynolds number for this simulation is $Re_b = 3285$ and the wall friction-based Reynolds number $Re_\tau = 110$. The domain size for this channel is $10.69h \times 2h \times 4h$ and $1920 \times 360 \times 720$ equidistant grid points are used to discretise the computational domain. The V-flame simulations are performed by placing a flame holder [3] in the fully developed channel flow at $y^+ = 55$ from the bottom wall (i.e. $y = 0.5h$). The simulation set-up for the V-flame is shown in Fig. 1. The boundary conditions are inflow with specified species mass fractions, density and velocity components at $x = 0$ and non-reflecting outflow at $x = 10.69h$ planes; no slip conditions are imposed at the walls. The boundaries in the z-direction are treated as periodic. The walls are assumed to be inert and impermeable, hence normal mass flux for all species is set to zero at the walls. The flame speed to friction velocity ratio $S_L/u_\tau = 0.7$. The simulations have been performed for approximately 3 flow-through times and the data has been sampled after 1 flow through time once the initial transience have decayed. The instantaneous flame structure represented by the $c = 0.5$ isosurface (where c is the normalised fuel mass fraction which increases monotonically from 0.0 in the unburned to 1.0 in fully burned products) for both wall conditions along with the normalised vorticity magnitude are shown in Fig. 1.

The head-on interaction (HOI) simulation in a turbulent boundary layer is performed by taking the solution from the fully developed turbulent channel flow up to $y/h = 1.33$ in all of the x and z directions. The domain size for this configuration is $10.69h \times 1.33h \times 4h$ which is discretised on $1920 \times 240 \times 720$ equidistant grid points. The boundary conditions for this case are imposed as periodic in the x and z directions and a mean streamwise pressure gradient is applied in the x direction to drive the flow. The boundaries in the $y-$direction are treated as wall at $y = 0$ where a no slip condition is imposed. An outflow boundary condition is specified at $y = 1.33h$. The initial flame is specified such that (e.g. $c = 0.5$

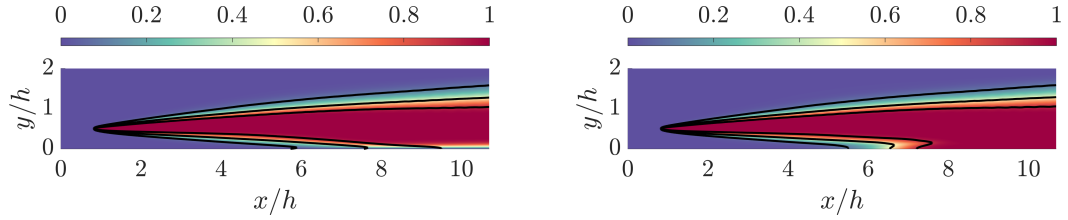

Isothermal Walls Adiabatic Walls

Figure 3: Favre mean non-dimensional temperature $\widetilde{T}$ along with the contour lines of the Favre mean progress variable at $\widetilde{c} = 0.1$, 0.5 and 0.9 for the V-flame OWI configuration with isothermal (top) and adiabatic (bottom) wall boundary conditions.

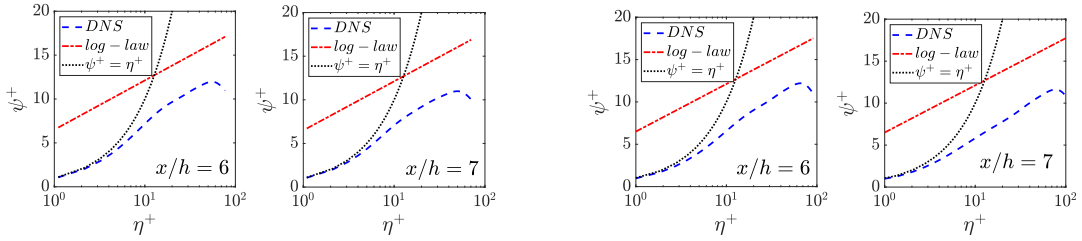

Isothermal Walls Adiabatic Walls

Figure 4: Profiles for ψ^+-vs-η^+ in the V-flame OWI configuration with isothermal walls (left) and adiabatic walls (right) at $x/h = 6$ and $x/h = 7$ near the bottom wall region.

is centred at $\approx 0.85h$) the reactant side of the flame is facing the wall, while the product side of the flame is facing the outflow boundary in the $y-$direction. Figure 2 shows the time evolution of the c = 0.5 isosurface at different time instants in the adiabatic and isothermal wall simulations.

2 RESULTS AND DISCUSSION

The non-reacting channel flow simulation has been compared with the results of [4] at $Re_\tau = 110$ and an excellent agreement has been obtained which has been reported in previous works [3, 2]. The variations of the Favre mean non-dimensional temperature, $\widetilde{T}$, and Favre mean progress variable, $\widetilde{c}$, in the V-flame OWI cases are presented in Fig. 3. The V-flame interacts with the wall further upstream in the case of adiabatic wall conditions when compared with the isothermal wall boundary condition, as shown in Fig. 3. This behaviour of the flame originates due to the differences in the temperature boundary condition at the wall and consequently due to the differences in the reaction rate values at the wall. It can be seen in Fig. 3 that under both wall boundary conditions the Favre mean non-dimensional temperature and progress variable fields remain coupled when the flame is away from the wall. As the flame approaches the isothermal wall there is decoupling between $\widetilde{T}$ and $\widetilde{c}$ fields whereas the temperature and progress variable remain coupled in the case of adiabatic wall boundary condition. Figure 4 shows the law of the wall for the two V-flame cases in terms of of $\eta^+ = \int_0^{y^+} (\nu_{wall}/\widetilde{\nu}) dy^+$ and $\psi^+ \int_0^{u^+} (\overline{\rho}/\rho_{wall}) du^+$ [5] where η^+ represents the density weighted y^+ and ψ^+ represents the density weighted u^+ to account for the density variation in the near wall region due to combustion. A significant deviation from the log-law can be seen at all the sampling locations in both of the V-flame cases due to a significant variation in density in the near wall region caused by heat release due to chemical reaction.

In the case of turbulent boundary layer HOI, the profiles for $\overline{\rho}$, $\widetilde{T}$, $\widetilde{Y}_F$ and $\widetilde{c}$ are presented in Fig. 5. It can be seen from Fig. 5 that the mean flame brush, represented by $\widetilde{c}$ distribution, becomes thicker due to interaction with the turbulence within the boundary layer and also propagates towards the wall as time progresses, eventually interacting with the wall. The flame eventually quenches due to heat loss at the wall in the case of isothermal wall and the reaction rate eventually vanishes due to the consumption of

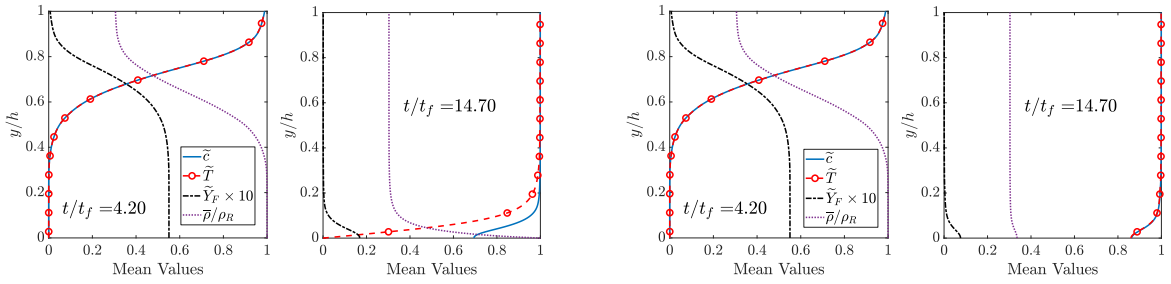

Isothermal Wall Adiabatic Wall

Figure 5: Profiles for $\widetilde{c}, \widetilde{T}, \overline{\rho}/\rho_R$ and $\widetilde{Y}_F \times 10$ in the turbulent boundary layer HOI configuration with isothermal walls (left) and adiabatic wall (right) at different time instants.

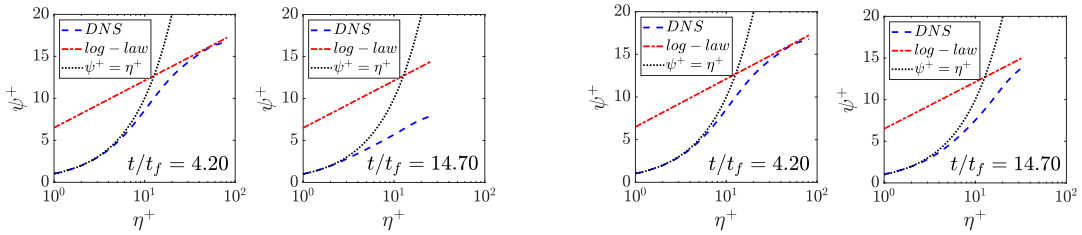

Isothermal Wall Adiabatic Wall

Figure 6: Profiles for ψ^+-vs-η^+ in the boundary layer HOI configuration with isothermal walls (left) and adiabatic walls (right) at different times.

reactants in the case of adiabatic wall. In this case at earlier time $t/t_f = 4.20$, there is no interaction of the flame with the wall hence the profiles for $\widetilde{T}$ and $\widetilde{c}$ are identical to each other under both wall boundary conditions. However, at later times (i.e. $t/t_f > 10.0$), the flame starts to interact with the wall under both wall boundary conditions and the differences in the $\widetilde{c}$ and $\widetilde{T}$ profiles start to appear for the isothermal wall boundary condition, whereas the $\widetilde{c}$ and $\widetilde{T}$ profiles remain identical in the case of the adiabatic wall. At this stage, the mean fuel mass fraction is considerably lower and consequently most of the domain is filled with hot burned gases which have a lower density as demonstrated by the difference in the distribution of $\widetilde{Y}_F$ at different times. Figure 6 shows the law of the wall for the two boundary layer HOI cases in terms of of η^+ and ψ^+. Similar to the V-flame cases a significant deviation in from the log-law is present at times when the flame is interacting with the wall which leads to density variations in the near wall region.

Understanding the fluctuations of scalars and their respective dissipation rates during FWI is not only necessary to be able to determine the thermal fatigue caused by intermittent temperature and unburned gas fluctuations in the near wall region [6], but is also needed for closing the mean reaction rate in the case of premixed turbulent combustion models [7]. The behaviours of the variance of the progress variable, $\widetilde{c''^2}$, and the variance of the non-dimensional temperature, $\widetilde{T''^2}$, in the near wall regions of the V-flame OWI cases under isothermal and adiabatic wall conditions are presented in Fig. 7 at $x/h = 6$ and $x/h = 7$. The differences between $\widetilde{c''^2}$ and $\widetilde{T''^2}$ in the case of isothermal wall exist due to the difference in the wall boundary conditions for c and T as explained earlier in the paper. In the case of isothermal boundary condition, the value of $\widetilde{T''^2}$ decreases to zero at the wall, as shown in Fig. 7, due to the value of the temperature imposed at the wall.

The behaviours of scalar dissipation rate of the progress variable, $\widetilde{\varepsilon}_c = \overline{\rho \alpha_c \nabla c'' \nabla c''}/\overline{\rho}$, where α_c is the diffusivity of the progress variable, and the scalar dissipation rate of the non-dimensional temperature, $\widetilde{\varepsilon}_T = \overline{\rho \alpha_T \nabla T'' \nabla T''}/\overline{\rho}$; α_T is the diffusivity of temperature, is investigated by comparing $\widetilde{\varepsilon}_c$ and $\widetilde{\varepsilon}_T$ at $x/h = 6$ and $x/h = 7$ for the V-flame OWI cases in Fig. 8. It can be noticed in Fig. 8 that in the case of

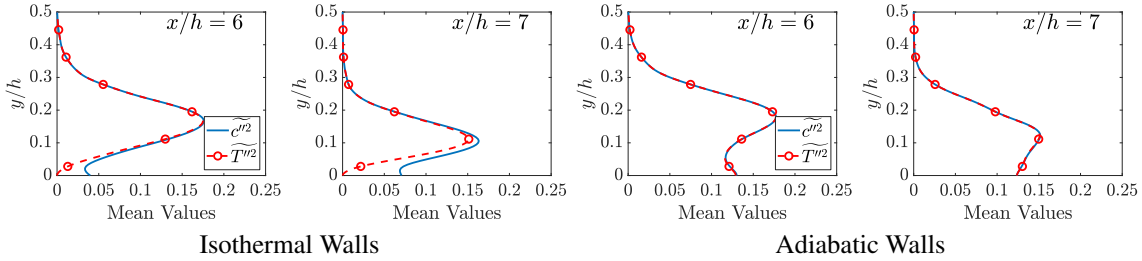

Figure 7: Profiles for $\widetilde{c''^2}$ and $\widetilde{T''^2}$ in the V-flame OWI configuration with isothermal walls (top) and adiabatic walls (bottom) at different locations downstream of the flame holder in the near wall region.

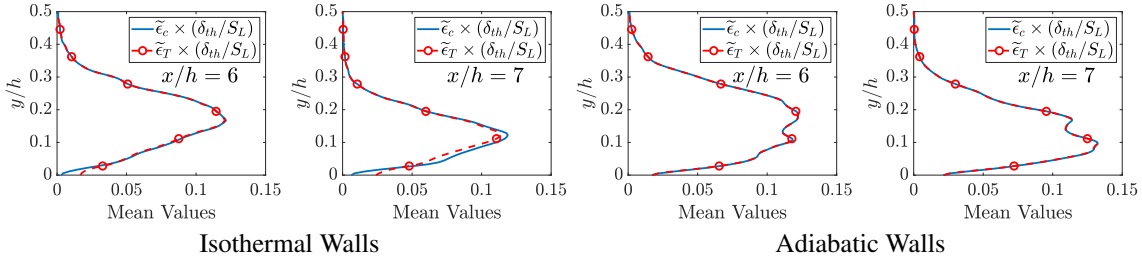

Figure 8: Profiles for $\widetilde{\epsilon}_c \times (\delta_{th}/S_L)$ and $\widetilde{\epsilon}_T \times (\delta_{th}/S_L)$ in the V-flame OWI configuration with isothermal walls (left) and adiabatic walls (right) at different locations downstream of the flame holder in the near wall region.

isothermal wall boundary condition, the values of $\widetilde{\epsilon}_T$ are higher than the values of $\widetilde{\epsilon}_c$ at the wall. This is due to the fact that the temperature field has a fixed value at the isothermal wall and as a consequence experiences much steeper gradients near the bottom wall when compared with the progress variable. In this case the mean flame brush represented by $\widetilde{c}$ broadens in the near wall region, as shown in Fig. 3, due to a low reaction rate as a consequence of wall heat loss and a high diffusion rate near the wall. In the case of adiabatic walls the values for $\widetilde{\epsilon}_c$ and $\widetilde{\epsilon}_T$ are identical at the wall due to no heat loss at the wall and a non-zero reaction rate at the wall. In this case the heat release due to chemical reaction enhances the gradients of the progress variable and temperature, especially in the wall tangential directions, leading to non-zero scalar dissipation rates at the wall.

Figure 9 shows the variation of $\widetilde{c''^2}$ and $\widetilde{T''^2}$ at different times during FWI in the turbulent boundary layer HOI cases. Under both wall boundary conditions $\widetilde{c''^2}$ and $\widetilde{T''^2}$ are identical when the flame is away from the wall at $t/t_f = 4.20$ as shown in Fig. 9. In the case of isothermal wall, as the flame propagates towards the wall, the differences between $\widetilde{c''^2}$ and $\widetilde{T''^2}$ start to increase in the near wall region. While in the case of an adiabatic wall the values for $\widetilde{c''^2}$ and $\widetilde{T''^2}$ remain identical, as shown in Fig. 9, which is consistent with the V-flame OWI case with adiabatic walls. The corresponding scalar dissipation rates for

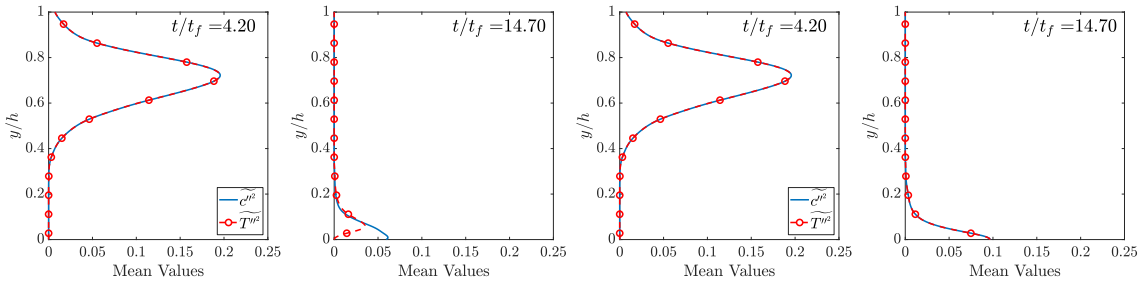

Figure 9: Profiles for $\widetilde{c''^2}$ and $\widetilde{T''^2}$ in the turbulent boundary layer HOI configuration with isothermal walls (left) and adiabatic wall (right) at different time instants.

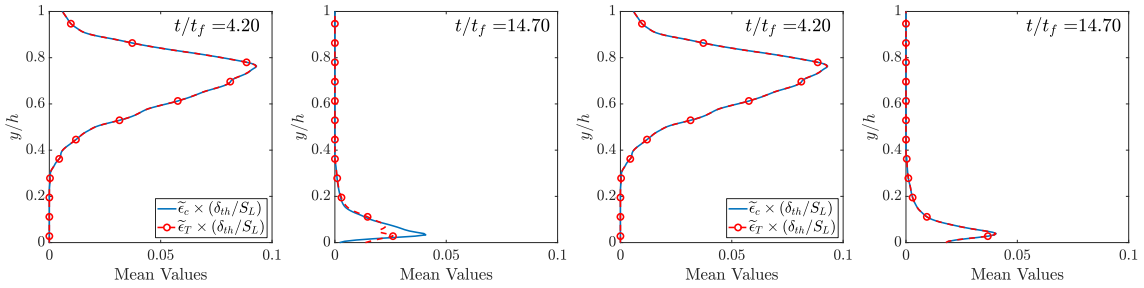

Figure 10: Profiles for $\widetilde{\varepsilon}_c \times (\delta_{th}/S_L)$ and $\widetilde{\varepsilon}_T \times (\delta_{th}/S_L)$ in the turbulent boundary layer HOI configuration with isothermal walls (left) and adiabatic wall (right) at different time instants.

$\widetilde{c''^2}$ and $\widetilde{T''^2}$ in the case of turbulent boundary layer HOI for both isothermal and adiabatic wall conditions are presented in Fig. 10. Similar to the V-flame OWI cases, the values for $\widetilde{\varepsilon}_T$ are much higher than $\widetilde{\varepsilon}_c$ during the FWI process with isothermal wall, as shown in Fig. 10, while the values for $\widetilde{\varepsilon}_c$ and $\widetilde{\varepsilon}_T$ are identical in the case of adiabatic wall.

3 CONCLUSIONS

Scalar statistics for two different turbulent flows in which flames interact with chemically inert isothermal as well as adiabatic walls in fully developed turbulent boundary layers have been investigated using DNS data for a friction velocity based Reynolds number, $Re_\tau = 110$. The main difference between the two configurations is the way the flames interact with the wall. Significant differences in the behaviour of the mean progress variable and the non-dimensional temperature have been observed between the two wall boundary conditions for both flow configurations. The mean scalar dissipation rates of progress variable and non-dimensional temperature decrease in the near wall region for both wall boundary conditions, but in the case of isothermal walls there is a decoupling between the two scalar dissipation rates and the scalar dissipation rate for non-dimensional temperature remains higher than the scalar dissipation rate for the progress variable. This variation in the scalar dissipation rates is a result of the steep temperature gradients introduced by the low temperature at the isothermal wall. The aforementioned statistics show that improved models are needed for accurate prediction of heat transfer and combustion behaviours in practical combustion devices.

ACKNOWLEDGEMENTS

The authors are grateful for the financial support from the EPSRC (Grant: EP/V003534/1). Computational support was provided by ARCHER, SuperMUC-NG, and the HPC facility at Newcastle University.

REFERENCES

[1] T. M. Alshaalan & C. J. Rutland. Turbulence, scalar transport, and reaction rates in flame-wall interaction. *Proc. Combust. Inst.*, **27** (1998) 793–799.

[2] U. Ahmed, N. Chakraborty, & M. Klein. Assessment of Bray Moss Libby formulation for premixed flame-wall interaction within turbulent boundary layers: Influence of flow configuration. *Combust. Flame*, **233** (2021) 111575.

[3] U. Ahmed, N. Chakraborty, & M. Klein. Scalar Gradient and Strain Rate Statistics in Oblique Premixed Flame-Wall Interaction Within Turbulent Channel Flows. *Flow, Turbul. Combust.*, **106** (2021) 701–732.

[4] T. Tsukahara, Y. Seki, H. Kawamura, & D. Tochio. DNS of turbulent channel flow at very low Reynolds numbers. In *Forth Int. Symp. Turbul. Shear Flow Phenom.*, pp. 935–940. Williamsburg, USA (2005).

[5] T. J. Poinsot & D. Veynante. *Theoretical and numerical combustion*. R.T.Edwards, Inc, 2nd edition (2005).

[6] K. Hanjalić & B. Launder. *Modelling Turbulence in Engineering and the Environment (Second-Moment Routes to Closure)*. Cambridge University Press (2011).

[7] K. N. C. Bray. The interaction between turbulence and combustion. *Seventeenth Symp. Symp. Combust.*, **17** (1979) 223–233.